

COMPARISON OF SINGLE CHANNEL POTASSIUM CURRENT IN BIOLOGICAL AND SYNTHETIC SYSTEMS — DEPENDENCE ON VOLTAGE*

ZUZANNA SIWY^a, SZYMON MERCIK^b, KARINA WERON^b,
REIMAR SPOHR^c, ALEXANDER WOLF^c AND ZBIGNIEW GRZYWNA^a

^aDepartment of Physical Chemistry and Technology of Polymers
Silesian University of Technology
Strzody 9, 44-100 Gliwice, Poland

^bInstitute of Physics, Wrocław University of Technology
Wybrzeże Wyspiańskiego 27, 50-370 Wrocław, Poland

^cGSI Darmstadt, Planckstr. 1, D-64291 Darmstadt, Germany

(Received January 10, 2000)

The influence of an external field on an ion current pattern in biological and synthetic systems was investigated. The patch clamp recordings of potassium current through a big conductance locust potassium channel (BK-channel) and a track-etched polyethylene terephthalate membrane were examined by the power spectrum, fractal analysis and relative dispersion analysis. A similar dependence of potassium current behaviour on the external voltage in both systems was found. The generalized dimension formalism is redefined to make it applicable to the analysis of time series.

PACS numbers: 87.22.-q, 05.40.+j

1. Introduction

Application of the patch clamp technique [1] into studies of ionic transport in purely synthetic membranes allowed to discover that single channel ion current fluctuations can also be observed beyond biological systems [2]. The time series of ionic current recorded in biological and synthetic systems look very similar. The ionic current continuously switches between various values corresponding to different states of the channel. The process is determined by the constantly varying environment, interactions between ions, ions and the channel, conformational changes of polymer forming a channel *etc.* High values of the current correspond to an “open” state, while the

* Presented at the XII Marian Smoluchowski Symposium on Statistical Physics Zakopane, Poland, September 6–12, 1999.

low ones to the “closed” state of the channel. The question, which appears in this context is whether the nature and characteristics of the measured currents is the same in both, entirely different groups of channels. Answering this question may help to pinpoint the physical processes, which are responsible for ion current fluctuations in both types of systems consisting of narrow conducting channels. Similarities and differences between ion currents through biological and synthetic membranes have already been pointed out by Pasternak *et al.*, and Grzywna *et al.* [3–5]. They found similar response of biological and synthetic membranes to divalent cations, protons and applied potential. In this paper we would like to continue the studies of the influence of voltage on the ion current properties in biological and synthetic systems by application of techniques, which may allow to get insight into the process occurring inside the pore. To characterize time series of potassium current we use the power spectrum, and also the fractal and relative dispersion analysis.

Track etched polyethylene terephthalate (PET) membrane was the synthetic system under study [6, 7]. The average diameter and length of the pore were approximately equal to 5nm and 10 μ m, respectively. Potassium current through a PET pore has been compared with potassium transport through the big conductance locust potassium channel [5].

2. Materials and methods

2.1. Synthetic membrane

The membrane examined was made of poly(ethylene terephthalate) (Hostaphan, PET) of a thickness of $10 \pm 1\mu$ m, that was irradiated with Kr ions and subsequently etched in hot alkali [6]. This treatment breaks the ester bonds (generating free carboxyl groups), and renders the pores hydrophilic. As a result of etching pores of average size of 5nm were formed in the membrane.

The membrane was placed in a Petri dish with 0.1M KCl solution buffered to pH=7 (see Fig. 1). The pipette (prepared with a Kopf model 730 pipette puller) filled with 1M KCl, pH=7, was approached to the membrane top using a micrometer screw. After establishing electric contact between the pipette tip and a pore of the membrane, the electric current through the pore was measured. The chosen value of pH corresponds to earlier observations of ion current through PET membranes [2], indicating that neutral pH favours current fluctuations.

Measurements of the ion current through the PET membrane were carried out at the Materials Research Department of GSI Darmstadt.

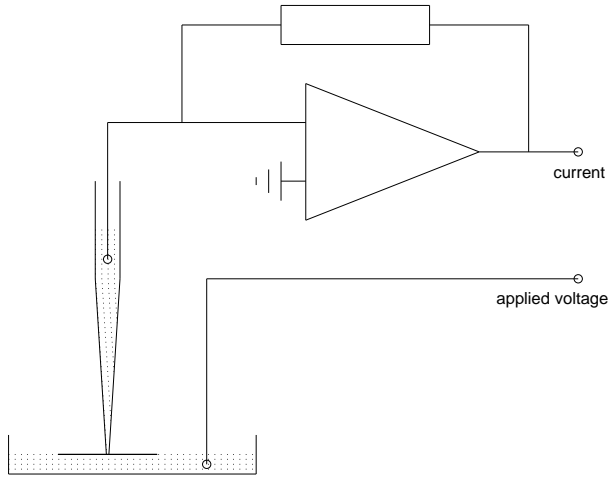


Fig. 1. Scheme of the experimental set up for measurements of the potassium current through PET pore [5].

2.2. Biological system

BK-channel data was recorded from cell attached patches of adult locust (*Schistocerca gregaria*) extensor tibiae muscle fibres [8]. The muscle preparation was bathed in 180mM NaCl, 10mM KCl, 2mM CaCl₂, 10mM 4-(2-hydroxyethyl)-1-piperazineethanesulphonic acid (HEPES), pH 6.8, and the patch pipettes contained 10mM NaCl, 180mM KCl, 2mM CaCl₂, 10mM HEPES, pH 6.8. Channel current was recorded using a List EPC-7 Patch-Clamp amplifier. Output was low-pass filtered at 10kHz, digitized at 22kHz using a Sony PCM ES-701 and stored on a videotape. Records were transferred to the hard disk of an IBM compatible PC via an analog-to-digital converter (Axon Instruments) sampling at 10kHz.

3. Results and discussion

3.1. Power spectrum

The power spectrum is one of the tools, which can give information about the character of an examined signal [9]. Application of its high frequency range into studies of the potassium current through a PET pore and a big conductance locust potassium channel, has already been shown in [5]. Power law scaling of the power spectrum detected in examined time series has suggested a non-Markovian nature of the ion transport, confirming the results obtained by the application of the Markov process definition [10].

The low frequency range of the power spectrum, as shown by Bezrukov [11], can also be used to examine the character of an ion current signal. The level of low frequency noise gives information about so called shot noise, a non-equilibrium noise, which is associated with current flow across a potential barrier. It is due to the fluctuation of current around an average value resulting from the discrete nature of a charge transfer [12,13]. The current spectral density of the shot noise is white (independent of the frequency) up to the frequency of the order of the inverse time of elementary charge transfer through the channel and is given by the Schottky's formula [11,12]:

$$S_I(f) = 2q\langle I \rangle, \quad (1)$$

where q is the transported charge, $\langle I \rangle$ — the average current. *Formula (1) is valid for any system, independent of its complexity, if the transfer of charge is unidirectional and charge transfer events are uncorrelated.* Only correlations between elementary steps of different charge carriers can change the low-frequency shot noise amplitude.

TABLE I

Comparison of shot noise (see Eq. (1)) and low-frequency noise of the power spectrum for **A** the BK channel and **B** the PET pore.

A	20mV	40mV	60mV	80mV	100mV	120mV
$S_I(f) = 2q\langle I \rangle$ $\left[\frac{\text{A}^2}{\text{Hz}} \right]$	$1.5 \cdot 10^{-30}$	$1.9 \cdot 10^{-30}$	$2.9 \cdot 10^{-30}$	$3.3 \cdot 10^{-30}$	$4.0 \cdot 10^{-30}$	$4.2 \cdot 10^{-30}$
noise level in the low frequency range of the power spectrum $\left[\frac{\text{A}^2}{\text{Hz}} \right]$	$1.1 \cdot 10^{-25}$	$6.3 \cdot 10^{-25}$	$1.6 \cdot 10^{-24}$	$4.7 \cdot 10^{-24}$	$1.2 \cdot 10^{-23}$	$6.6 \cdot 10^{-24}$
B	0V	-1V	-2V	-3V	-4V	-5V
$S_I(f) = 2q\langle I \rangle$ $\left[\frac{\text{A}^2}{\text{Hz}} \right]$	$4.8 \cdot 10^{-32}$	$9.8 \cdot 10^{-31}$	$7.0 \cdot 10^{-30}$	$1.5 \cdot 10^{-29}$	$3.2 \cdot 10^{-29}$	$7.0 \cdot 10^{-29}$
noise level in the low frequency range of the power spectrum $\left[\frac{\text{A}^2}{\text{Hz}} \right]$	$1.0 \cdot 10^{-35}$	$5.0 \cdot 10^{-33}$	$1.0 \cdot 10^{-31}$	$5.0 \cdot 10^{-31}$	$8.0 \cdot 10^{-31}$	$1.0 \cdot 10^{-30}$

Examination of the noise level in the low-frequency range of the power spectrum enables to detect a deterministic component in a system. Table I shows values of the shot noise, calculated according to Eq. (1) for the high conductance locust potassium channel (A) and PET pore (B), together with the low frequency noise of the power spectra.

As it can be seen from the table the significant difference (several orders of magnitude) between values of the shot noise and the low frequency noise of the power spectrum indicates the existence of correlations in all examined time series and, therefore, a deterministic component in the investigated systems [11].

3.2. Fractal dimension

Self-similarity of a time series means that a property $L(t)$ measured at the time scale t is proportional to that property measured at the time scale at [14,15]

$$L(at) = kL(t), \quad (2)$$

where $k = a^{d_T - d_F}$ is the proportionality parameter, d_T is a topological dimension, d_F is a measure of the self-similarity in time, for a discrete time series $a \in \mathbf{N}$. We have selected every n -th (odd or even) point of an original set, and have drawn it versus time as it would correspond to measurements at different sampling frequencies. We point here at the difference between the fractal dimension of an attractor in a pseudo-phase phase [16] and the fractal dimension of a time series calculated from Eq. (2).

In our study of the experimental data we have defined $L(t)$ as:

1. The total charge Q_{tot} transported through the pore over time t , equal to the integral of the ion current $I(t)$; for a discrete time series, the total charge is equal to:

$$L(t) \equiv Q_{\text{tot}}(t) = \sum_{i=1}^{N-1} \frac{1}{2} (I_i + I_{i+1}) \Delta t.$$

N — length of the time series, Δt is defined by the sampling frequency; $N \cdot \Delta t = t$.

2. The total length of the current time series ℓ_{tot} ; in this case we treat $I(t)$ as a geometrical object

$$L(t) \equiv \ell_{\text{tot}}(t) = \sum_{i=1}^{N-1} \sqrt{(\Delta t)^2 + (I_{i+1} - I_i)^2}.$$

As it can be seen from Fig. 2, the fractal dimension calculated on the basis of the total transported charge is not sensitive to the external voltage and equals 1. It means that the charge flow is directly proportional to time and the information of the total transported charge is independent of the sampling frequency. The examined process, therefore, is surprisingly regular

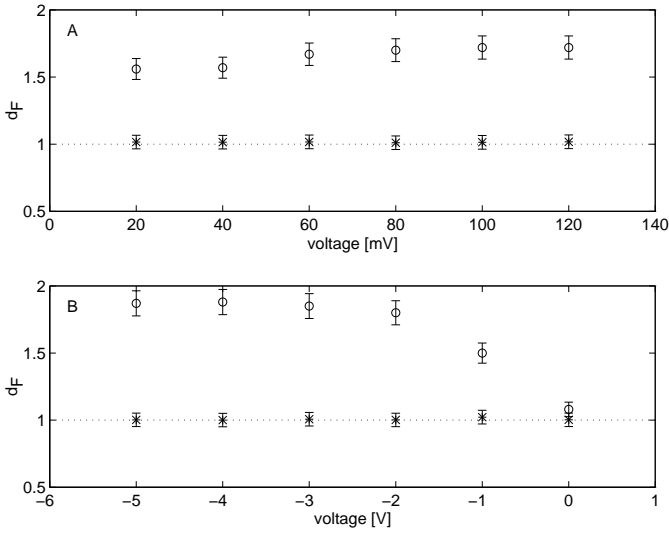


Fig. 2. Fractal dimension found from Eq. (2) for the potassium current time series recorded at different voltages **A** for the BK channel, **B** for the PET pore. $L(t)$ has been equal to the total charge transported through the channel (stars) or to the total length of the function $I(t)$ (circles).

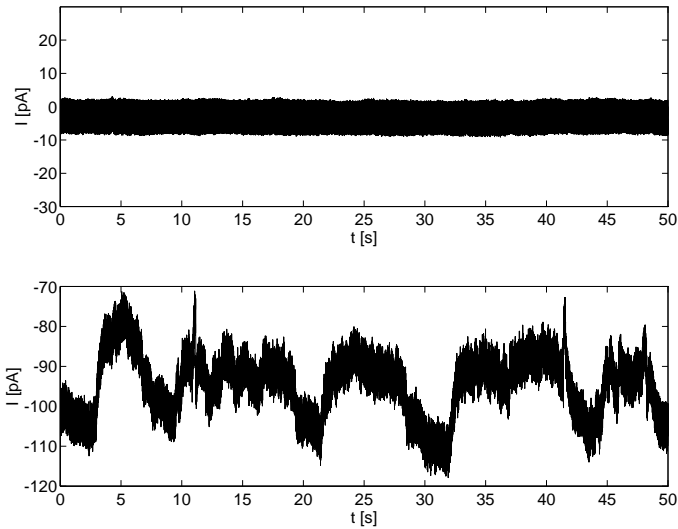


Fig. 3. Time series of K^+ current through PET pore recorded at -1 V (top) and -4 V (bottom) with 1 kHz sampling frequency.

from the point of view of the total transported charge over prolonged time, in contrast to the chaotic behaviour of ionic current — the local rate of the charge transport. Figure 2 shows also that analysis of the self-similar properties of the time series, treated as geometrical objects, allowed to differentiate between recordings obtained at different voltages. Higher fractal dimensions for higher voltages indicate formation of more complex ionic current fluctuations at stronger external field applied. As it can be seen in Fig. 3, for low voltage the signal is “silent”, while high voltage induces openings and closings of the pore.

3.3. Generalized dimension formalism

As the fractal dimension alone could not clearly distinguish between time series we asked the question whether the generalized dimension, which characterizes an object with a set of numbers, provides a better way of the time series description. The generalized dimension D_q of an object has been defined as [16, 17]

$$D_q = \lim_{\varepsilon \rightarrow 0} \frac{1}{1-q} \frac{\ln \sum_{i=1}^{M(\varepsilon)} P_i^q}{\ln \varepsilon} \quad (3)$$

where P_i , $i = 1, 2, \dots$, is the probability of finding an element of the object in the i -th element of covering, ε defines the scale of covering, $M(\varepsilon)$ is a number of covering elements at the scale ε , q is a real number.

To apply the notion of the generalized dimension into the analysis of time series, the set $\{P_i\}$ had to be re-defined accordingly. We were interested in the self-similarity in time, therefore, we could not use the standard methods leading to the analysis of an attractor in the pseudo-phase space [16]. The set $\{P_i\}$ has been defined in two different ways corresponding to two approaches for calculation of d_F used in the previous section. The total time T of recordings has been divided into N equal segments of length τ and $\{P_i\}$ could be defined in two ways:

1. The charge flowing through the pore in the given time segment τ_i , divided by the total transported charge:

$$P_i = \frac{Q(\tau_i)}{\sum_{j=1}^n Q(\tau_j)}, \quad i = 1, 2, \dots \quad (4)$$

2. The length of the curve $I(t)$ in the given time segment divided by its total length

$$P_i = \frac{\ell(\tau_i)}{\sum_{j=1}^n \ell(\tau_j)}, \quad i = 1, 2, \dots \quad (5)$$

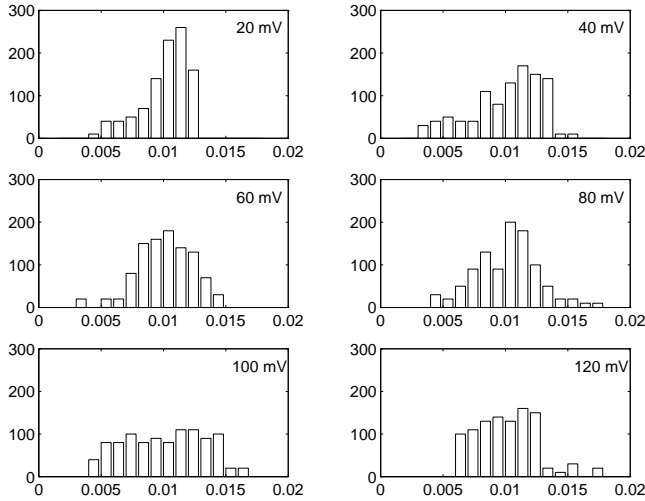


Fig. 4. Histograms of $\{P_i\}$ distribution (Eq. (4)) for the potassium current through the big conductance locust potassium channel for different voltages. The y -axis presents the normalized frequency. The $\{P_i\}$ set has been defined on the basis of the total charge transported through the channel.

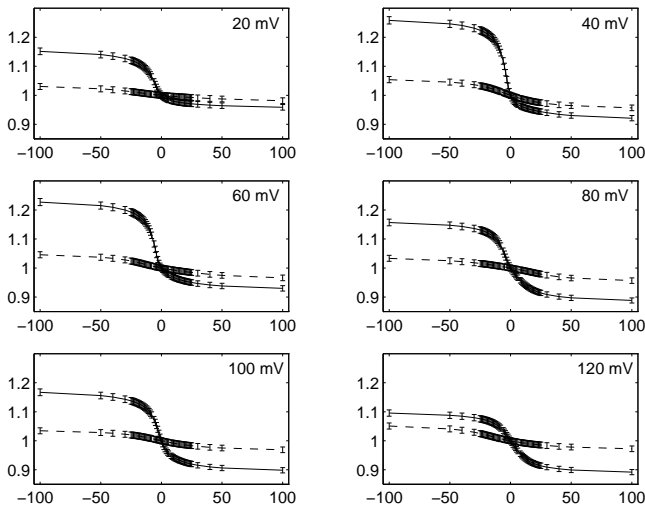


Fig. 5. Generalized dimension found on the basis of the total transported charge for the potassium current through the BK channel (D_q , solid line) and for its surrogates (\tilde{D}_q , dashed line). The x -axis presents q . Voltages are indicated in the Figure. Note, that D_q found from Eq. (3) gives D_0 equal to 1. The curves for \tilde{D}_q are not significantly different from one another.

The set of probabilities $\{P_i\}$ is the key quantity in Eq. (3), therefore, we have looked at first at their distribution. Figure 4 presents the normalized histogram of probabilities $\{P_i\}$, calculated on the basis of the total transported charge, for ion current in the BK system at different voltages. The width of the histogram is a measure of heterogeneity of subsequent time segments from the point of view of the total transported charge. For low voltages the histogram is narrow, getting wider with increasing applied voltage. For the highest applied voltage (120mV) the histogram becomes narrow again. The way, in which the $\{P_i\}$ distribution influences the generalized dimension can be followed in Fig. 5. The dependence of the width of D_q values range on the applied voltage is similar to the relation found for the width of the $\{P_i\}$ histogram (see Table IIA). To check whether the D_q formalism is sensitive to the character of the data the same analysis has been performed for the surrogates of the K^+ current experimental data. The surrogates have been obtained by the random shuffling of all the data positions [15]. As it can be seen from Fig. 5 the general pattern, observed for the original current data, is lost. According to the earlier studies [18], for low voltages the influence of a stochastic force (originating *e.g.* from thermal motion) on the system behaviour is very strong, therefore, the narrowness of the $\{P_i\}$ distribution as well as the D_q values is due to the predominance of the stochastic nature of the system. For higher voltages, the closed and open states become more distinct, which results in the widening of the $\{P_i\}$ and D_q ranges. For even higher voltage the ionic current behaviour is governed by a deterministic force, and subsequent time segments become again more homogeneous.

The same analysis has been done for the K^+ current through a single pore in the PET membrane. Figure 6 shows normalized histograms of the probabilities $\{P_i\}$ calculated on the basis of the total transported charge at different voltages. As it can be seen from Figs. 6 and 7 the same dependence of the system behaviour on external voltage has been found for the synthetic pore as it was observed in a BK channel (see also Table IIB). Figure 7 presents also the monofractal character of D_q found for surrogates of potassium current through the PET pore — the dependence of \tilde{D}_q on q and an applied voltage does not exist.

The generalized dimension D_q is a very slowly changing function, defined for an infinite domain, therefore, it is often more convenient to examine the Legendre's transform of the function: $\tau_q = D_q(1 - q)$, so called $f(\alpha)$ relation [16] where

$$\alpha = \frac{\partial \tau}{\partial q} \quad (6)$$

and D_q is defined by Eq. (3). The relation $f(\alpha)$ corresponding to D_q func-

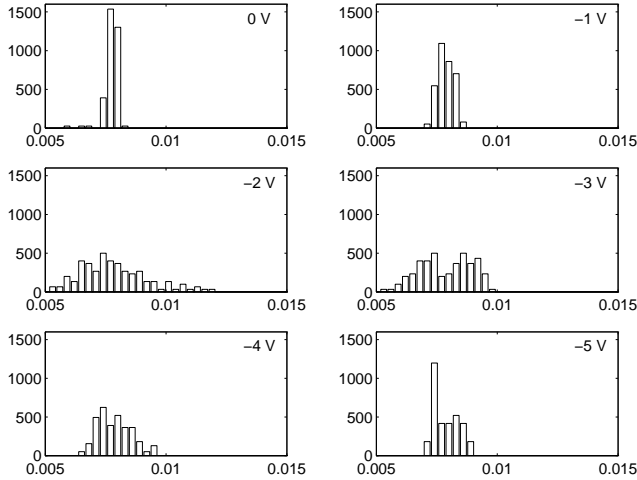


Fig. 6. Histograms of $\{P_i\}$ distribution (Eq. (4)) for the potassium current through the PET track-etched membrane. The y -axis presents the normalized frequency. The $\{P_i\}$ set has been defined on the basis of the total charge transported through the channel.

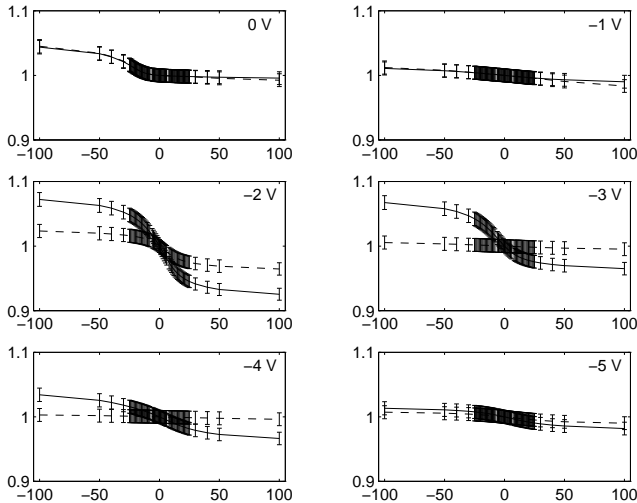


Fig. 7. Generalized dimension found on the basis of the total transported charge for the potassium current through the PET pore (D_q , solid line) and for its surrogates (\tilde{D}_q , dashed line). The x -axis presents q . Voltages are indicated in the Figure. Note, that D_q found from Eq. (3) gives D_0 equal to 1. The curves for \tilde{D}_q are not significantly different from one another.

TABLE II

Differences between D_{-100} and D_{100} for the potassium current through **A** the BK channel and **B** the PET pore, for different voltages. D_q has been calculated on the basis of the total transported charge (see Figs. 5 and 7).

A	20mV	40mV	60mV	80mV	100mV	120mV
$D_{-100} - D_{100}$	0.20 ± 0.02	0.34 ± 0.02	0.30 ± 0.02	0.27 ± 0.02	0.27 ± 0.02	0.20 ± 0.02
B	0V	-1V	-2V	-3V	-4V	-5V
$D_{-100} - D_{100}$	0.05 ± 0.01	0.02 ± 0.01	0.15 ± 0.01	0.10 ± 0.01	0.07 ± 0.01	0.03 ± 0.01

tions (and \tilde{D}_q for the surrogates data) for the current through BK channel presented in Fig. 5 is shown in Fig. 8, and the relation for the current through the PET pore presented in Fig. 7 is shown in Fig. 9. The range of α corresponds to the range of D_q (\tilde{D}_q) values.

Figure 10 presents the normalized histogram of the probabilities $\{P_i\}$ calculated on the basis of the length of ionic current function for the BK system at different voltages, while Fig. 11 shows the corresponding D_q relation. As it can be seen from the figures, for higher voltage the wider widths of the histogram and the range of D_q values are observed. That shows quantitatively the formation of stronger ionic current fluctuations at stronger external fields. The pattern is lost for surrogates data (Fig. 11). The dependence of the width of D_q values range on the applied voltage is similar to the relation found for the width of the $\{P_i\}$ histogram (see Table III).

TABLE III

Differences between D_{-100} and D_{100} for the potassium current through **A** the BK channel; **B** the PET pore for different voltages. D_q has been calculated on the basis of the total length of $I(t)$ function (see Figs. 11 and 12).

A	20mV	40mV	60mV	80mV	100mV	120mV
$D_{-100} - D_{100}$	0.07 ± 0.02	0.31 ± 0.02	0.36 ± 0.02	0.41 ± 0.02	0.43 ± 0.02	0.42 ± 0.02
B	0V	-1V	-2V	-3V	-4V	-5V
$D_{-100} - D_{100}$	0.00 ± 0.01	0.01 ± 0.01	0.00 ± 0.01	0.01 ± 0.01	0.00 ± 0.01	0.01 ± 0.01

The generalized dimension D_q for the PET pore has appeared to be a constant, which suggests its monofractal character (Figs. 9 and 12). The big difference in the D_q relation obtained for synthetic and biological systems may result from the differences in their structure. The synthetic pore is around 10 times larger and its length is 10 to 50 thousand times greater than the length of a biological ion channel. The potassium current signals

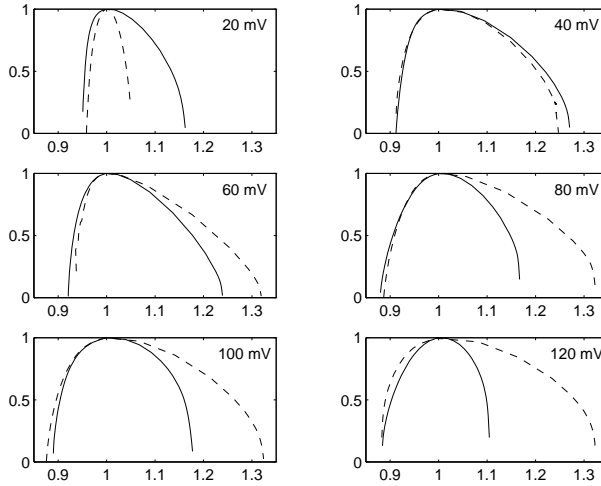


Fig. 8. $f(\alpha)$ relation for the potassium current through the BK channel, for voltages as indicated in the Figure. The solid line corresponds to the generalized dimension D_q shown in Fig. 5, obtained on the basis of the total transported charge. The dashed line is related with the D_q relation found on the basis of the total length of $I(t)$ relation (shown in Fig. 11).

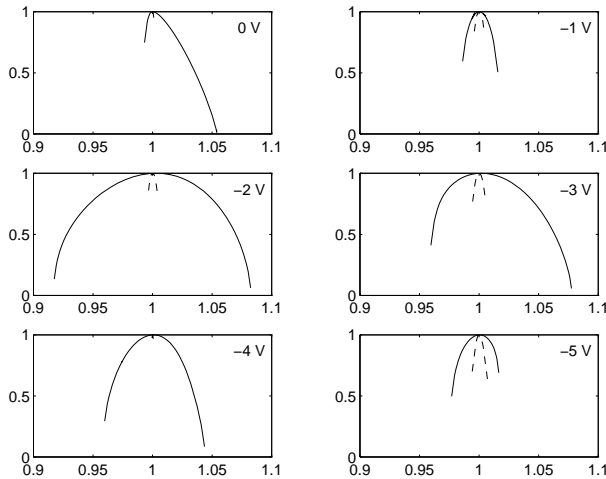


Fig. 9. $f(\alpha)$ relation for the potassium current through the PET pore, for voltages as indicated in the Figure. The solid line corresponds to the generalized dimension D_q shown in Fig. 7, obtained on the basis of the total transported charge. The dashed line is related with the D_q relation found on the basis of the total length of $I(t)$ relation (shown in Fig. 12).

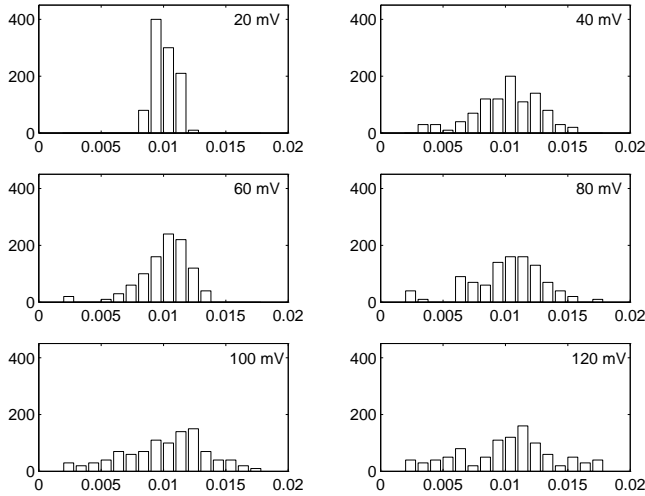


Fig. 10. Histograms of $\{P_i\}$ distribution (Eq. (5)) for the potassium current through the big conductance locust potassium channel. The y -axis presents the normalized frequency. The $\{P_i\}$ set has been defined by the total length of $I(t)$ function.

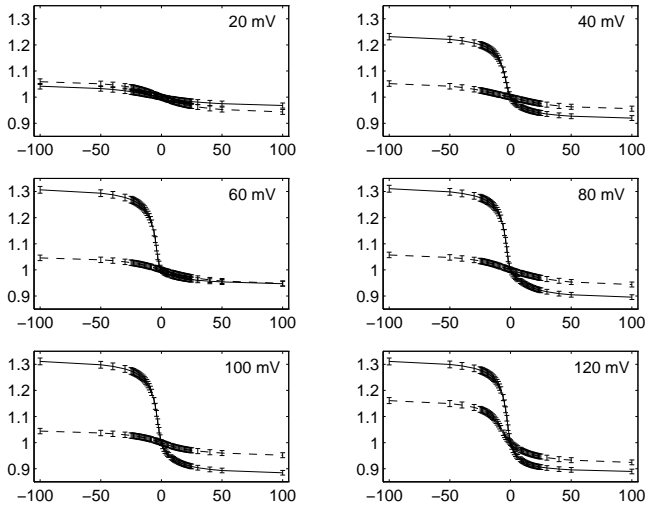


Fig. 11. Generalized dimension found on the basis of the total length of ionic current function for the potassium current through the BK channel (D_q , solid line) and for its surrogates (\tilde{D}_q , dashed line). The x -axis presents q . Voltages are indicated in the Figure. Note, that D_q found from Eq. (3) gives D_0 equal to 1. The distinct curve for \tilde{D}_q was obtained for surrogates of the current recorded at 120 mV.

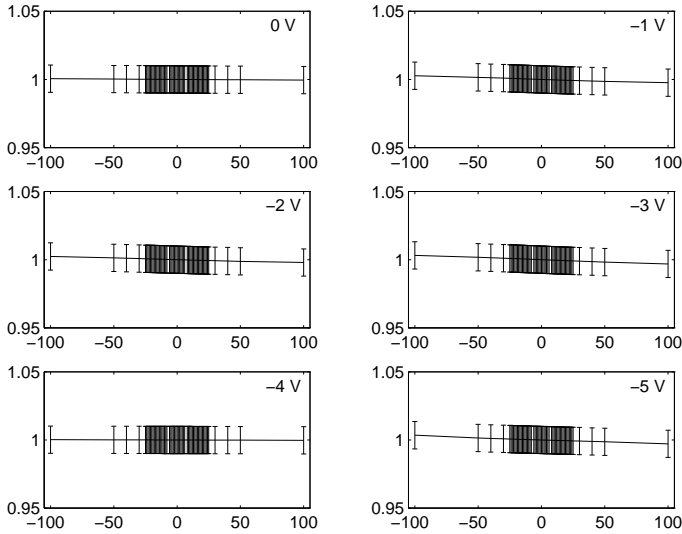


Fig. 12. Generalized dimension found on the basis of the total length of the $I(t)$ function for the potassium current through the PET pore, at the voltages as indicated in the Figure. Note, that D_q found from Eq. (3) gives D_0 equal to 1.

recorded at the synthetic system may, therefore, carry less structural information than those of biological channels, simply due to an averaging during much longer time of transport.

3.4. Relative dispersion analysis

Power law scaling of the power spectrum, the transported charge and the length of ionic current function suggests the self-similarity in time of the examined time series. To assess their temporal heterogeneity we had, therefore, to apply scale-independent techniques. Relative dispersion (RD) analysis, which covers a wide range of scale, is one of them [9]. RD is defined as a quotient of the standard deviation and the mean of an examined property. It scales with the sample's size m as

$$\frac{RD(m)}{RD(m_0)} = \left(\frac{m}{m_0} \right)^{1-D}, \quad (7)$$

where m_0 is an arbitrary chosen reference time interval. For a discrete time series recorded with a given sampling frequency f_s , m_0 is usually chosen as $1/f_s$. D is a dispersion exponent called also a fractal dimension, which gives insight into the nature of the data. $D = 1.5$ represents random, uncorrelated data, $D = 1$ indicates uniformity of examined property over all length scales [9].

As it can be seen from Table IV the scaling exponent D , found from Eq. (7), is significantly different for the BK channel and the PET pore. The result may suggest higher heterogeneity and faster changes of the ionic current in biological systems. Exponent D does not distinguish, however, between time series recorded at different voltages.

TABLE IV
Local dispersion exponent calculated from Eq. (5) for the potassium current through **A** the BK channel and **B** the PET pore.

A	20mV	40mV	60mV	80mV	100mV	120mV
dispersion exponent D	1.20 ± 0.02	1.19 ± 0.02	1.20 ± 0.02	1.20 ± 0.02	1.15 ± 0.02	1.20 ± 0.02
B	0V	-1V	-2V	-3V	-4V	-5V
dispersion exponent D	1.03 ± 0.01	1.03 ± 0.01	1.02 ± 0.01	1.02 ± 0.01	1.01 ± 0.01	1.01 ± 0.01

4. Concluding remarks

The main objective of the paper was to compare character and self-similar properties of the ion transport in biological and synthetic channels systems. We have examined potassium current through the big conductance locust potassium channel and the track-etched PET pore. Low-frequency range of the power spectrum shows the existence of correlation in all examined time series, suggesting their non-Markovian character. Self-similarity in time of K^+ current signal has been examined through application of homogeneous function. Fractal dimension estimated on the basis of the total transported charge and the length of $I(t)$ function depends on the external voltage in a similar way for both types of membranes. To provide a better description of the self-similar character of the examined time series a re-defined generalized dimension D_q and $f(\alpha)$ formalism have been used. The range of D_q function (and α), in which $\{P_i\}$ have been defined as a fraction of the total transported charge, in both cases of the potassium current through BK channel and PET pore, increases with an increasing voltage, and at higher voltages it becomes narrow again. This result may suggest an ordering influence of voltage on the transport of charges through the pore, which has already been shown by surrogate data, generalized entropy, and pseudo-phase portraits analysis [18]. D_q function calculated on the basis of the total length behaves for BK channel differently - its range becomes wider with the increase of the applied field, while the PET signal, in this case, has been found monofractal. We would like to emphasize that in any attempts of the physical interpretation of the data, it is important to treat the signal as the result of interactions within the whole system consisting of the channel

and the ions. A biological channel is narrower, therefore, one could expect, that ions going through can “feel” the channel structure stronger than in the case of a PET pore. The biological signal contains hence more structural information and is more “complex” itself, which is also seen in the higher value of the local dispersion exponent.

Finally, we would like to emphasize that only by parallel application of several techniques, which take up different aspects of the examined phenomenon, it is possible to learn about its nature and properties [10, 19, 20].

REFERENCES

- [1] E. Neher, B. Sakmann, *Sci. Am.* **266**, 44 (1992).
- [2] C.A. Pasternak, C.L. Bashford, Y.E. Korchev, T.K. Rostovtseva, A. Lev, *Colloids Surf.* **77**, 119 (1993).
- [3] C.A. Pasternak, G.M. Alder, P.Y. Apel, C.L. Bashford, D.T. Edmonds, Y.E. Korchev, A.A. Lev, G. Lowe, M. Milovanovich, *Radiat. Meas.* **25**, 675 (1995).
- [4] C.A. Pasternak, G.M. Alder, P.Y. Apel, C.L. Bashford, Y.E. Korchev, A.A. Lev, T.K. Rostovtseva, N.I. Zhitariuk, *Nucl. Instrum. Methods Phys. Res., Sect. B* **105**, 332 (1995).
- [5] A. Wolf, Z. Siwy, Y.I. Korchev, N. Reber, R. Spohr, *Cell. Mol. Biol. Lett.* **4**, 553 (1999).
- [6] R. Spohr, *Ions Tracks and Microtechnology. Principles and Application*, Friedr. Vieweg & Sohn Verlagsgesellschaft mbH, Braunschweig 1990.
- [7] Z.J. Grzywna, Z. Siwy, C.L. Bashford, *J. Membr. Sci.* **121**, 261 (1996).
- [8] M.S.P. Sansom, F.G. Ball, C.J. Kerry, R. McGee, R.L. Ramsey, P.N.R. Usherwood, *Biophys. J.* **56**, 1229 (1989).
- [9] J. Bassingthwaighte, L. Liebovitch, B. West, *Fractal Physiology*, Oxford University Press, New York 1994.
- [10] A. Fuliński, Z. Grzywna, I. Mellor, Z. Siwy, P.N.R. Usherwood, *Phys. Rev.* **E58**, 919 (1998).
- [11] S.M. Bezrukov, I. Vodyanoy, in *Advances in Chemistry Series Biomembrane Electrochemistry*, **235**, M. Blank, I. Vodyanov, eds., American Chemical Society, Washington DC. 1994.
- [12] W. Schottky, *Ann. Phys. (Berlin)* **57**, 541 (1918).
- [13] H.W. Ott, *Noise Reduction Techniques in Electronic Systems*, John Wiley & Sons, New York 1976.
- [14] Z.J. Grzywna, L.S. Liebovitch, Z. Siwy, *Cell. Mol. Biol. Lett.* **2**, 4 (1997).
- [15] L.S. Liebovitch, *Fractals and Chaos Simplified*, Oxford University Press, New York 1998.
- [16] H.G. Schuster, *Deterministic Chaos*, 3rd edn., VCH Verlagsgesellschaft, Weinheim 1988.

- [17] T. Tel, *Z. Naturforsch.* **43a**, 1154 (1988).
- [18] Z. Siwy, Z.J. Grzywna, *Cell. Mol. Biol. Lett.* **4**, 525 (1999).
- [19] Sz. Mercik, K. Weron, Z. Siwy, *Phys. Rev.* **E60**, 7343 (1999).
- [20] Sz. Mercik, Z. Siwy, K. Weron, *Physica* **A276**, 376 (2000).